FLOW CHARACTERISTICS OF A 40-INCH WIND TUNNEL AT MACH NUMBERS 1.5 TO 6

By

Jack D. Coats

von Kármán Gas Dynamics Facility

ARO, Inc.

a subsidiary of Sverdrup and Parcel, Inc.

June 1962

ARO Project No. 330225

ABSTRACT

The flexible steel plate which forms the lower nozzle wall of the 40-in. Supersonic Tunnel of the von Kármán Gas Dynamics Facility was damaged in October 1961. A brief description of the damage and repair of the plate is presented with flow characteristics obtained during a calibration program conducted after completion of the repairs. The calibration showed that the uniformity of the test-section flow characteristics was not adversely affected by the repair which included the use of a pattern of bolt heads protruding above the surface of the plate in the subsonic region of the nozzle.

CONTENTS

TABLE

ILLUSTRATIONS

NOMENCLATURE

K	Flow angularity factor, $\Delta p/\alpha_F p_o$, $\Delta p/\beta_F p_o$, 1/deg
M	Local Mach number
M_c	Nozzle contour Mach number
M_p	Centerline Mach number measured by the retractable sidewall probe
M_∞	Mean centerline Mach number
Δp	Pressure difference across cone surface, psia
p_o	Stilling chamber pressure, psia
p_{o1}	Pressure downstream of a normal shock wave, psia
Re	Reynolds number per inch
X, Y, Z	Tunnel axes (Fig. 4b)
x, y, z	Coordinates along X, Y, and Z axes, respectively, in.
α_F	Flow angle in X, Z plane (Fig. 4b), deg
β_F	Flow angle in X, Y plane (Fig. 4b), deg
δ	Boundary-layer total thickness, in.
δ^*	Boundary-layer displacement thickness, in.

1.0 INTRODUCTION

The flexible steel plate which forms the lower nozzle wall in the 40-in. Supersonic Tunnel of the von Kármán Gas Dynamics Facility (VKF), Arnold Engineering Development Center (AEDC), Air Force Systems Command (AFSC), USAF, was damaged on October 10, 1961. The damage (Fig. 1) occurred in the converging region of the nozzle upstream of the throat where several of the lugs, which connect the flexible plate to actuators 47 through 51 (opposite actuators 7 through 11 on the top plate), were broken or cracked. The plate was removed from the tunnel, and the five rows of damaged lugs (eight lugs per row) were replaced. Unlike the original lugs, which were machined as an integral part of the plate, each of the replacements was attached to the plate with four bolts which extend through the plate with the heads protruding 0.158 in. above the plate surface (Fig. 1). Details of the replacement lugs are presented in Fig. 2. After installation of the repaired plate, the tunnel was ready for operation on December 7, 1961.

Since the flexible nozzle plate had to be reset, thereby introducing the possibility of moderate changes in the nozzle contour, and an assessment of the aerodynamic effects of the repair was required, the tunnel was calibrated prior to resumption of testing. An investigation of test-section Mach number and flow-angle distributions at each half Mach number from 1.5 to 5 and at Mach number 6 was conducted during the period from December 7 to December 27, 1961. Testing at Mach number 6 was temporarily curtailed after several failures of the seals between the flexible plates and the tunnel sidewalls. Further calibration at Mach number 6 on January 26, 1962, after the cause of the seal failure was corrected, included measuring the centerline Mach number distribution and correlating the mean centerline Mach number with a reference Mach number measured at a fixed tunnel station by a retractable sidewall probe.

Oil flow studies were made at Mach numbers 1.5 and 5 to determine the effects of the bolt head pattern on the flow in the boundary layer in the subsonic region of the nozzle. Boundary-layer velocity profiles were measured in the test section on the curved wall of the nozzle at Mach numbers 1.5 and 5 on January 19, 1962, to provide data for comparison with boundary-layer characteristics obtained prior to the tunnel repair.

Manuscript released by author June 1962.

This report is intended primarily to provide current Mach number and flow-angle data which supersede that presented in the previous tunnel calibration report (Ref. 1).

2.0 APPARATUS

2.1 WIND TUNNEL

The 40-in. Supersonic Tunnel is a continuous, closed-circuit, variable-density wind tunnel with a Mach number range from 1.5 to 6. The top and bottom walls of the nozzle are flexible plates, which are automatically positioned at desired contours by electrically driven screwjacks. Calculated contours are available at Mach numbers 1.5 to 2.5 in. increments of 0.25 and up to Mach number 6 in increments of 0.5. In addition to these contours, the nozzle control system provides for setting interpolated contours at intermediate Mach numbers. Thus far, calibrations have been made at Mach numbers 1.5 to 5 in 0.5 increments and at Mach number 6. Models are generally mounted on a sector which rotates in the horizontal plane, providing angular displacements from -5 to +15 deg.

The stilling chamber is equipped with a cheesecloth filter and eleven fine-mesh turbulence damping screens. The tunnel is driven by a 93,000-horsepower compressor system which provides maximum tunnel stagnation pressures from 29 psia to 200 psia at Mach numbers 1.5 and 6, respectively (Fig. 3). Minimum operating pressures are less than one-tenth of the maximum. A 7550-cu-ft, 4,000-psia dry-air storage system and a 200,000-cu-ft vacuum sphere allow rapid changes of the operating pressure level to produce various test Reynolds numbers. Below Mach number 5 the tunnel is normally operated with a stagnation temperature of 100°F. This temperature can be raised to 300°F to prevent liquefaction at the higher Mach numbers. The absolute humidity of the tunnel air can be maintained below 0.0001 lb of water per lb of air (dew point of -35°F at atmospheric pressure) by large capacity silica gel driers.

2.2 TEST EQUIPMENT

A calibration rake (Fig. 4a) consisting of five cones spaced at 6-in. intervals was used to obtain flow angularity and Mach number distributions. Each cone was constructed with four equally spaced static orifices on the cone surface for measuring flow angularity and a pitot orifice for evaluating Mach number at the apex of the cone.

The rake and attached instrument package (Fig. 4a) were traversed through the test section with a hydraulically operated probe carrier system.

The rake was not used during a second calibration at Mach number 6 because installation of the carrier mechanism requires extensive dismantling of the tunnel. Instead, a single pitot probe supported by a sector-mounted probe carrier was used to determine the centerline Mach number distribution. Also during this entry a reference Mach number (M_p) on the tunnel centerline at station x = +33 in. was measured with the retractable sidewall probe shown in Fig. 4b. This probe which has been permanently installed on the tunnel sidewall is intended primarily to eliminate the uncertainty in Mach number during extended high temperature operation at Mach number 6. This type of operation has been found to introduce shifts in the level of the Mach number while having relatively no effect on the Mach number distribution. The Mach number measured by the retractable probe may therefore be directly related to the mean centerline Mach number and thereby provides a means of evaluating the mean centerline Mach number during normal tunnel operation.

The boundary-layer rake shown in Fig. 4b was used to obtain the test-section boundary-layer characteristics on the upper and lower nozzle walls.

2.3 INSTRUMENTATION AND DATA REDUCTION

Flow angularity measurements were made with transducers which measured the differential pressures between the static orifices located in the pitch and in the yaw planes. The rake pitot pressures were obtained with a reference pressure system consisting of a single transducer, referenced to a vacuum, which measured the common reference pressure and individual transducers which measured the variations of each of the pitot pressures from the reference pressure level. During the second calibration at Mach number 6, the pitot pressures of both the traversing centerline probe and the retractable sidewall probe were measured with transducers referenced to a vacuum. Transducers utilizing a vacuum reference were also used to measure the pitot pressures obtained with the boundary-layer rake.

Mach numbers were obtained from the stilling chamber to pitot pressure ratio (p_o/p_{o_1}) with the following equation:

$$M = \frac{-\left[a_o + a_1(p_o/p_{o_1}) + a_2(p_o/p_{o_1})^2 + a_3(p_o/p_{o_1})^3 + a_4(p_o/p_{o_1})^4\right]}{b_o + b_1(p_o/p_{o_1}) + b_2(p_o/p_{o_1})^2 + b_3(p_o/p_{o_1})^3 + b_4(p_o/p_{o_1})^4}$$

Values of $a_o \ldots a_4$ and $b_o \ldots b_4$ are given in Table 1.

Flow angles were obtained from the differential pressures with the relationship:

$$\alpha_F \text{ or } \beta_F = \Delta p/p_o K$$

The values of K for each Mach number were obtained from experimental and theoretical data presented in Ref. 1.

Data reduction was accomplished with the VKF ERA-1102 digital computer. Automatic data plotters and tabulators were used to obtain the Mach number and flow-angle distributions in both graphical and tabular form. The overall uncertainties in the Mach number and flow angles are estimated to be ±0.004 and ±0.05 deg, respectively.

3.0 PROCEDURE

The nozzle settings for all Mach numbers were obtained from the theoretical contours. At Mach numbers from 2 to 6 the flow angularity and Mach number distributions were measured along the nozzle centerline and at ±6 in. and ±12 in. in the horizontal and vertical planes. At Mach number 1.5, a 6-in. interval is not adequate to eliminate interference between the cones; therefore, the cones located at ±6 in. (Fig. 4) were removed. These cones were replaced with pitot tubes, thus providing Mach number data at ±6 in. for a portion of the test at M_c = 1.5 and during check runs at Mach numbers from 2 to 6.

Data were obtained at 2.5-in. intervals over a 55-in. region of the test section extending from station x = -18 in. to station x = +37 in. (Fig. 1). Measurement of the flow characteristics at each Mach number were made at Reynolds numbers corresponding to near the maximum tunnel stagnation pressure and at three reduced pressure levels. These test conditions are shown on the plot of tunnel operating conditions presented in Fig. 3.

Testing at Mach number 6 was temporarily curtailed after several failures of the seals between the flexible plate and the sidewalls. The cause of the seal failure was corrected; however, further calibration

at Mach number 6 was delayed until installation of the retractable sidewall probe was completed. The second calibration at Mach number 6 included obtaining the centerline Mach number distribution and determining the relationship between the mean centerline Mach number and a reference Mach number measured by the retractable sidewall probe. Data were again obtained at four stilling chamber pressures (Fig. 3); however, the survey was limited by the sector-supported probe carrier to a 44-in. region extending from station x = -13 in. to station x = +31 in.

4.0 RESULTS

The possibility of the bolt heads creating a disturbance in the subsonic region of the nozzle, which could in turn affect the test-section flow characteristics, was examined prior to repair of the flexible plate. Theoretical estimates (Refs. 2 and 3) of the local Mach number and the boundary-layer total and displacement thickness in the subsonic region of the nozzle are presented in Fig. 5. At Mach number 5 the bolt heads are in a region of low local Mach number and are followed by a marked increase in flow velocity which results in a large favorable pressure gradient. These factors in conjunction with the thick boundary layer in the area of the bolt heads indicate that the test-section flow characteristics may be relatively unaffected by the bolt pattern. It is evident that the conditions are considerably less favorable at Mach number 1.5 where the boundary-layer thickness is greatly reduced and the bolt pattern lies in a region of relatively high Mach number followed by a significantly smaller, although still favorable, pressure gradient.

Fluorescent oil was used to obtain a visual indication of the effects of the bolt pattern on the subsonic flow. Flow patterns around the bolt heads in the converging region of the nozzle at Mach numbers 1.5 and 5 are presented in Fig. 6. At Mach number 1.5 where the theoretical estimates indicated that bolt head interference was most likely, the data show that all bolt heads created disturbances in the flow, while at Mach number 5 the disturbances were limited to the two rows of bolt heads at the downstream end of the bolt pattern.

The effects of the bolt head pattern are further illustrated in Fig. 7 where the test-section boundary-layer displacement thickness obtained from velocity profile measurements made on the curved walls at Mach numbers 1.5 and 5 are compared with data obtained prior to the tunnel repair. At Mach number 5 the test-section boundary-layer

displacement thicknesses are essentially the same on the top and bottom walls and are also in good agreement with previous measurements. At Mach number 1.5, however, the displacement thickness on the bottom plate (measurements were not made on the top plate at $M_c = 1.5$) is considerably greater than values from previous investigations (Ref. 4).

As was mentioned previously, the tunnel sector rotates in the horizontal plane. The Mach number distributions in the horizontal plane are therefore of primary importance since they are most representative of the region normally occupied by models. The local Mach number distributions along the tunnel centerline and at ±6 in. and ±12 in. in the horizontal plane are presented in Fig. 8 for nominal Mach numbers from 1.5 to 5. The data presented were generally obtained at the maximum Reynolds number. It was found that within this Mach number range, variations in Reynolds number result primarily in a shift in the level of the Mach number and do not significantly affect the distribution. These data are therefore considered representative of the Mach number distributions at all Reynolds numbers. The plots show that the variations of the local Mach number in the horizontal plane are relatively small, i.e. generally $< \pm 0.01$.

A general increase in the mean centerline Mach number with Reynolds number and the maximum variations of the local Mach number within the central region of the test section (±6 in. and ±12 in. off-axis in the horizontal and vertical planes throughout the 55-in. region surveyed) are illustrated in Fig. 9. The chart (Fig. 9a) shows that the maximum variation of the local Mach number is generally ±0.5 percent or less except at Mach number 1.5 where the variations reach ±0.9 percent.

The variations of the local Mach number and the sidewall probe reference Mach number from mean centerline values at various Reynolds numbers at Mach number 6 are illustrated in Fig. 10a. It should be noted that the sector-supported probe carrier droops somewhat below the tunnel centerline at the fully extended position, thereby introducing the differences in Mach number indicated at station x = +33 in. The data show a significant effect of Reynolds number on the Mach number distribution. This is reflected in the maximum variation of the local centerline Mach number which increases from ±0.3 percent at $Re \geq 0.19 \times 10^6$ to ±0.5 percent at $Re = 0.08 \times 10^6$. The Reynolds number influence is summarized in Fig. 10b by the Mach number 6 correlation factor ($M_\infty - M_p$) which relates the mean centerline Mach number and the reference Mach number measured with the retractable probe.

The test-section flow-angle characteristics at Mach numbers from 1.5 to 5 are summarized in Fig. 11. The mean values of the flow angles along the tunnel centerline in both the pitch and yaw planes are generally less than 0.15 deg. Maximum variations of the centerline flow angles are largest in the yaw plane at low Mach numbers (±0.2 deg) and gradually decrease with increasing Mach number. Maximum flow-angle variations within the central region of the test section range from approximately ±0.3 deg at low Mach numbers to a maximum of ±0.56 deg in the pitch plane at Mach number 5. The increase in the off-axis flow angles in pitch plane with increasing Mach number is caused by the boundary-layer growth along the parallel tunnel sidewalls.

5.0 CONCLUDING REMARKS

A calibration of the 40-in. Supersonic Tunnel was conducted at Mach numbers from 1.5 to 6 after completion of the repairs on the damaged lower flexible plate. The effects of a bolt pattern in the converging region of the nozzle were investigated locally with fluorescent oil studies and in the test section by obtaining boundary-layer velocity profile measurements. The following remarks are based on these investigations:

1. The maximum variation of the local Mach number within the region surveyed was ±0.9 percent at Mach number 1.5 and generally ±0.5 percent or less at Mach numbers from 2 to 5.
2. Maximum variation of the local centerline Mach number at Mach number 6 was ±0.3 percent at $Re > 0.19 \times 10^6$.
3. Average flow angles along the test-section centerline decrease with increasing Mach number and are generally less than 0.15 deg with maximum centerline flow-angle variations not exceeding ±0.2 deg.
4. The uniformity of the test-section flow characteristics appears to be relatively unaffected by the bolt heads in the subsonic region of the nozzle.

REFERENCES

1. Schueler, C. J. and Strike, W. T. "Calibration of a 40-Inch Continuous Flow Tunnel at Mach Numbers 1.5 to 6." AEDC-TN-59-136, November 1959.

2. Tucker, M. "Approximate Turbulent Boundary Layer Development in Plane Compressible Flow Along Thermally Insulated Surfaces with Application to Supersonic-Tunnel Contour Correction." NACA Technical Note 2045, March 1950.

3. Sibulkin, M. "Boundary Layer Measurements at Supersonic Nozzle Throats." Journal of Aeronautical Sciences, Vol. 24, April 1957, pp. 249-252.

4. Jones, J. "An Investigation of the Boundary Layer Characteristics in the Test Section of a 40 by 40-in. Supersonic Tunnel." AEDC-TN-60-189, October 1960.

TABLE 1

CONSTANTS USED IN MACH NUMBER CALCULATIONS

$$M = \frac{-\left[a_o + a_1 (p_o/p_{o1}) + a_2 (p_o/p_{o1})^2 + a_3 (p_o/p_{o1})^3 + a_4 (p_o/p_{o1})^4\right]}{b_o + b_1 (p_o/p_{o1}) + b_2 (p_o/p_{o1})^2 + b_3 (p_o/p_{o1})^3 + b_4 (p_o/p_{o1})^4}$$

For $1.45 \leq M_c \leq 4.00$:

a_o	1.001610×10^0	b_o	1.559619×10^{-1}
a_1	-3.650480×10^0	b_1	8.774662×10^{-1}
a_2	1.911036×10^0	b_2	-1.042554×10^0
a_3	9.538176×10^{-1}	b_3	-1.693207×10^{-1}
a_4	0	b_4	1.221138×10^{-3}

For $4.00 \leq M_c \leq 8.3$:

a_o	9.987988×10^{-1}	b_o	-1.201229×10^0
a_1	2.413334×10^0	b_1	-6.284801×10^{-1}
a_2	2.050745×10^{-1}	b_2	-3.179190×10^{-2}
a_3	2.030949×10^{-3}	b_3	-1.856653×10^{-4}
a_4	7.040420×10^{-11}	b_4	7.040420×10^{-8}

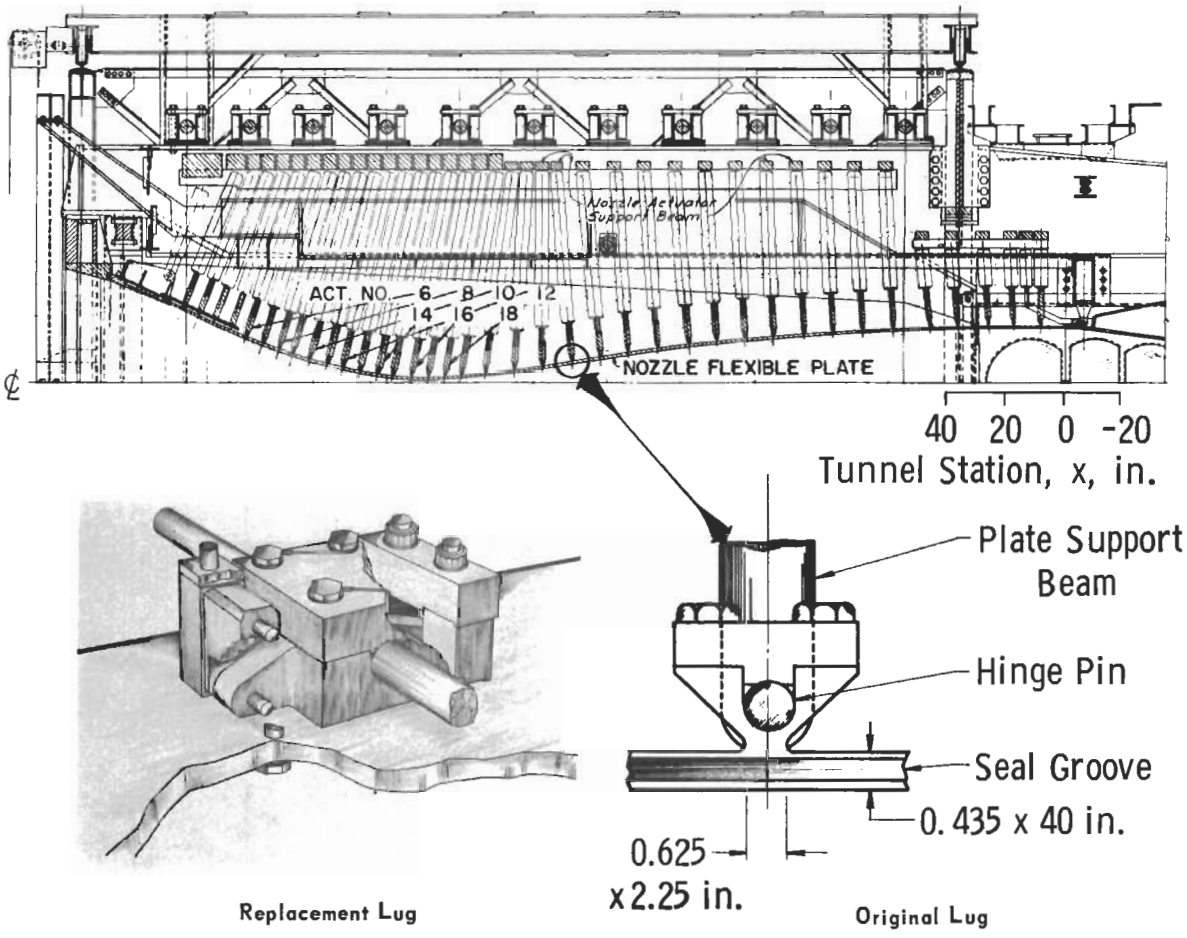

Fig. 1 The 40-in. Supersonic Tunnel

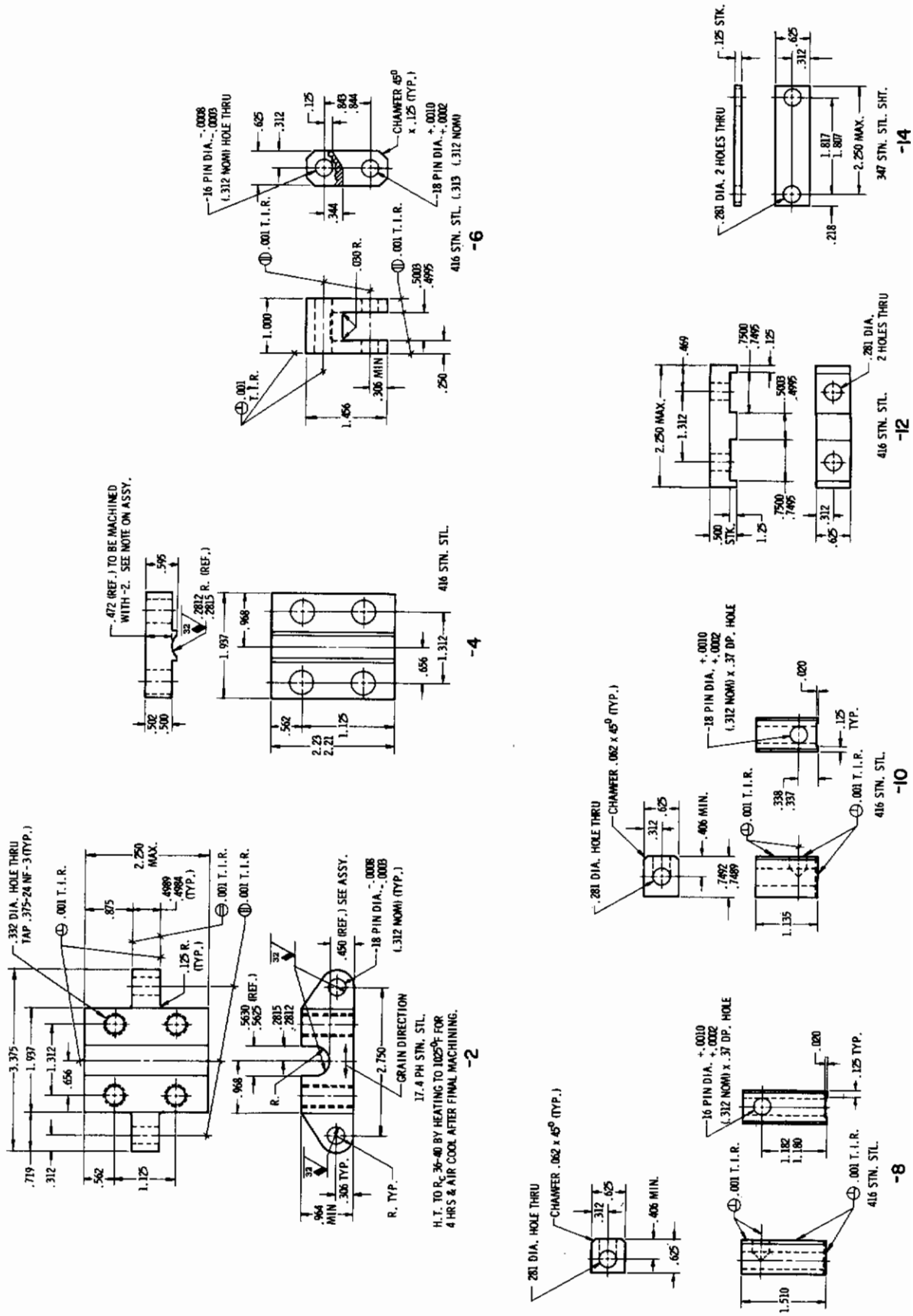

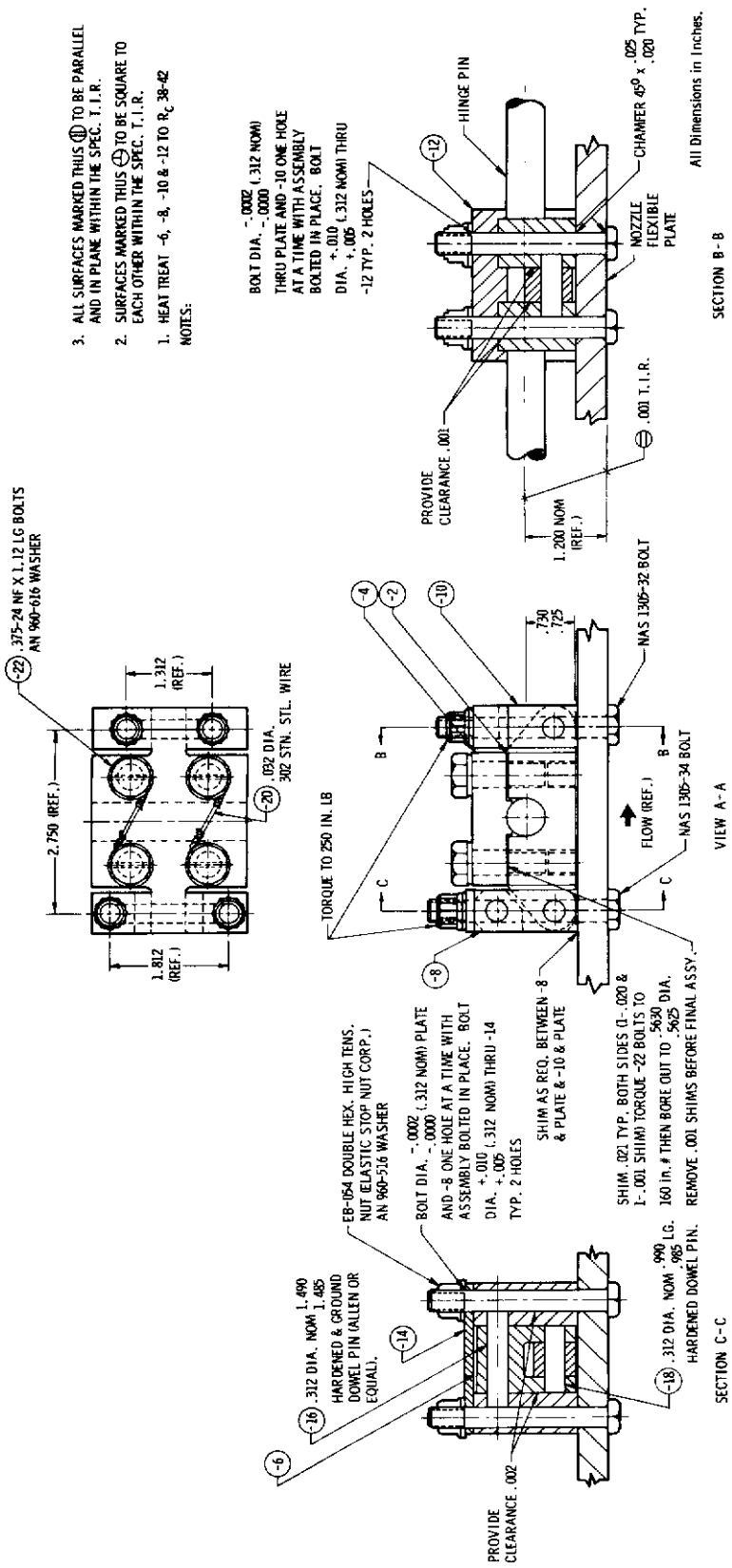

Fig. 2 Replacement Lug Details

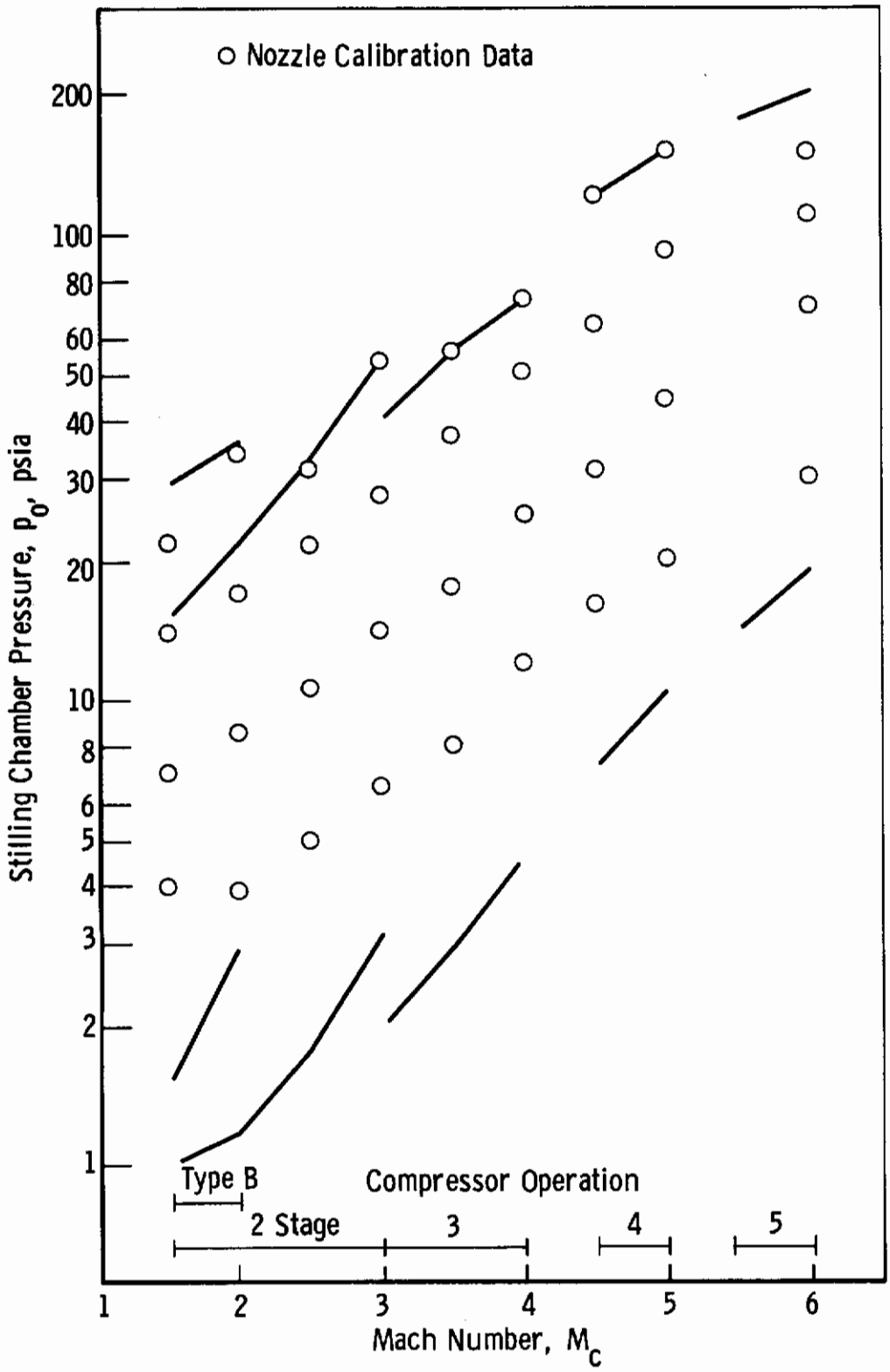

Fig. 3 Tunnel Operating Pressures and Calibration Test Conditions

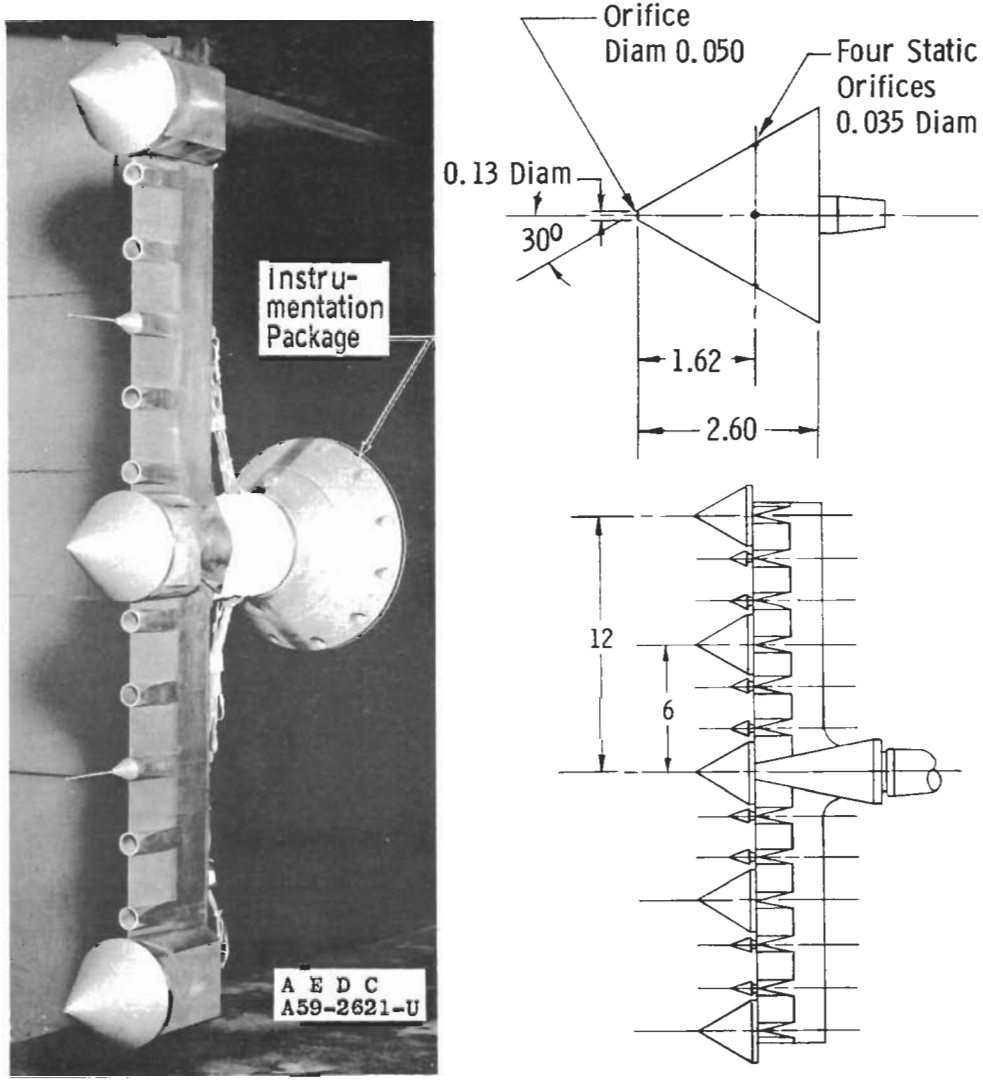

a. Calibration Rake and Probes

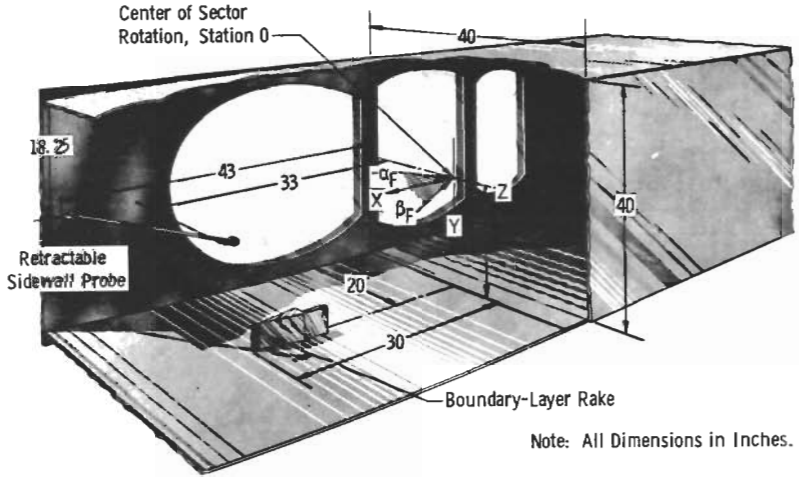

b. Retractable Sidewall Probe and Boundary-Layer Rake

Fig. 4 Test Equipment

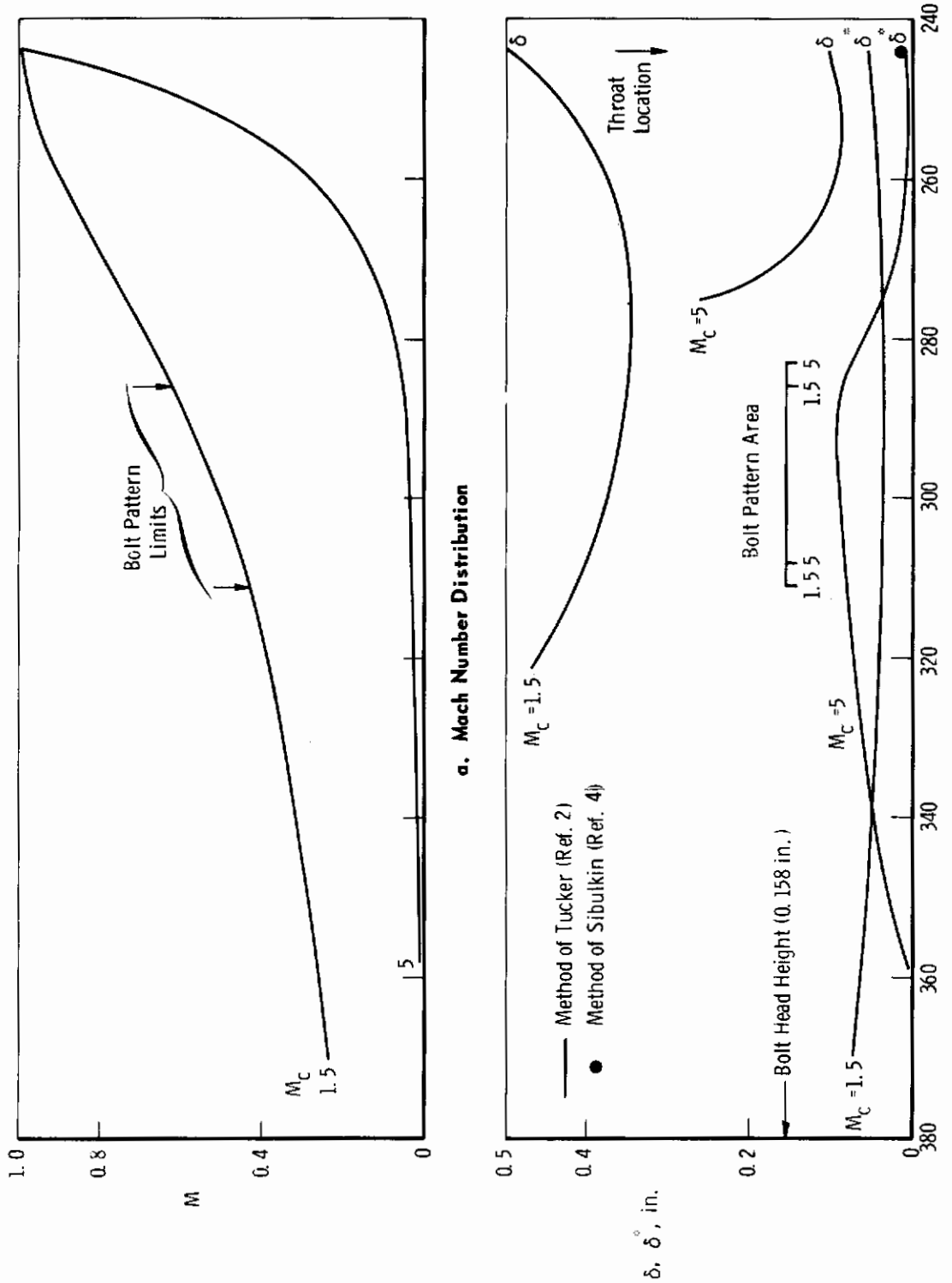

a. Mach Number Distribution

b. Boundary-Layer Total and Displacement Thickness

Fig. 5 Subsonic Section Characteristics

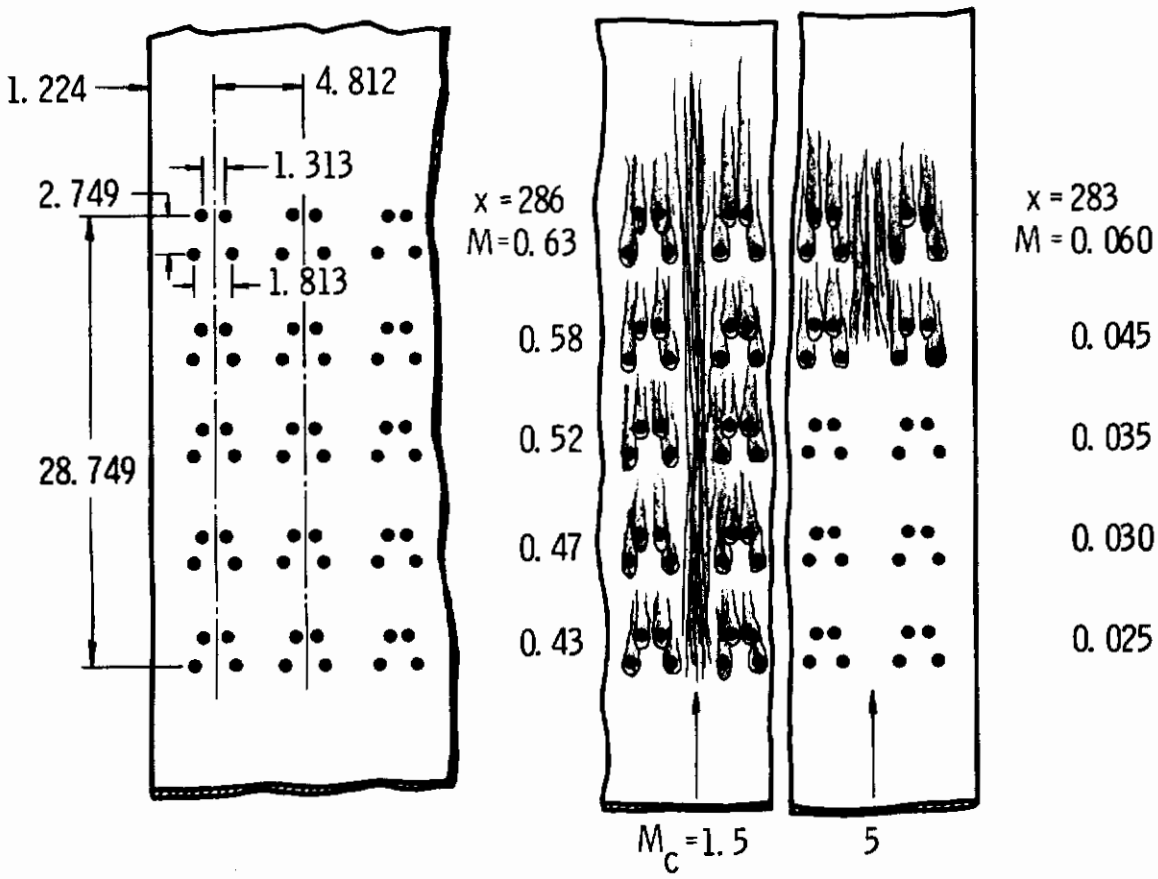

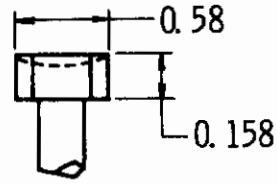

Bolt Head Geometry
Hex Head NAS 1305

All dimensions in inches.

Fig. 6 Bolt Pattern and Streamlines at M_c = 1.5 and 5

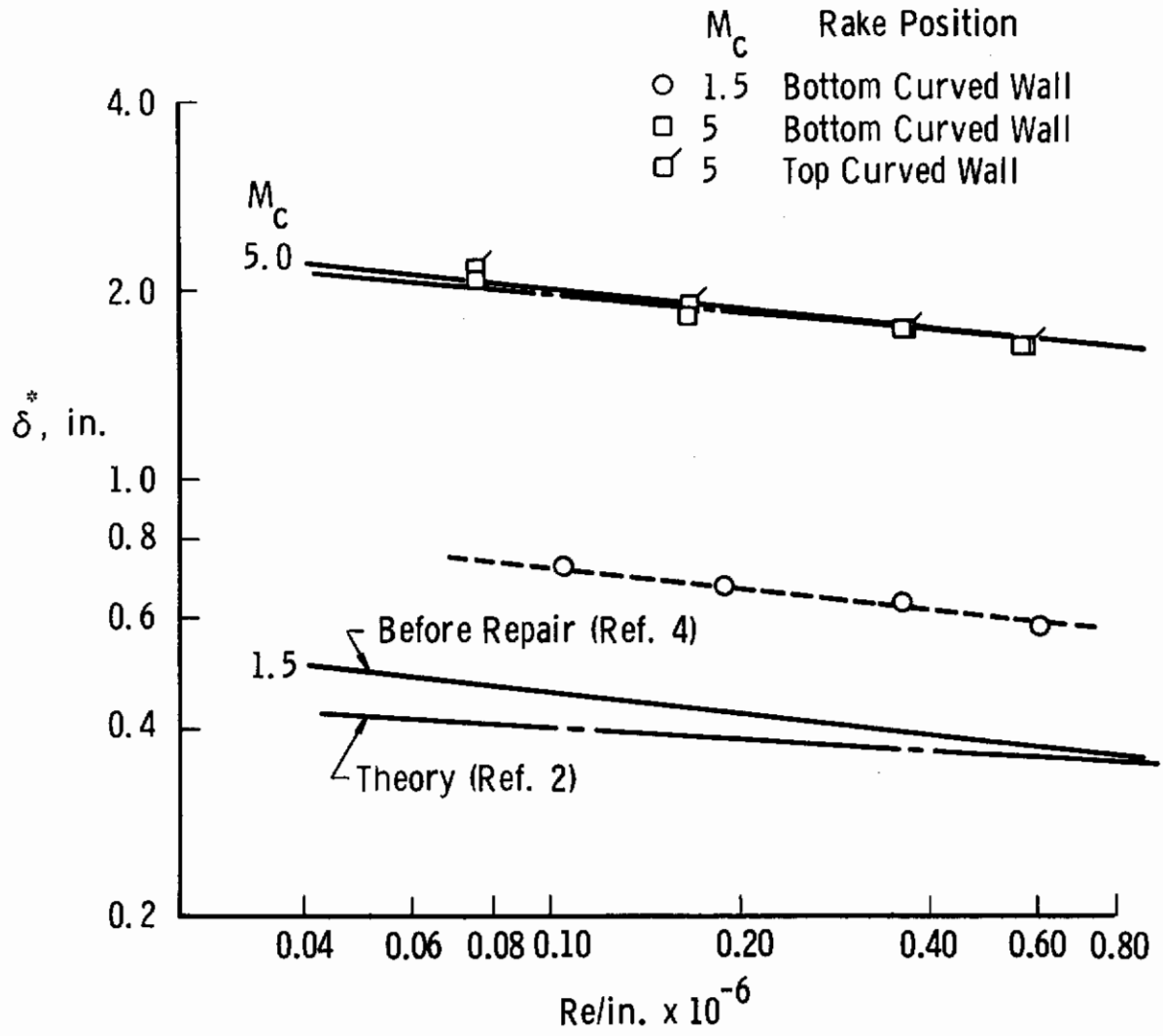

Fig. 7 Displacement Thickness on Curved Wall, M_c = 1.5 and 5

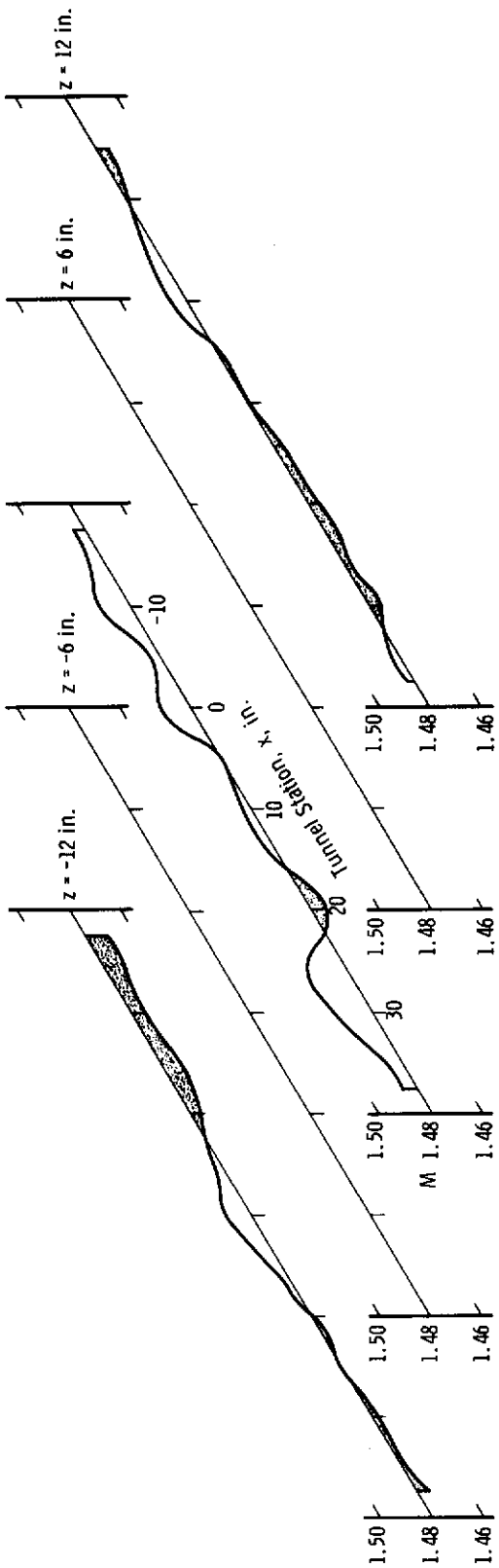

a. $M_c = 1.5$, $Re = 0.53 \times 10^6$

Fig. 8 Mach Number Distribution in the Horizontal (Pitch) Plane

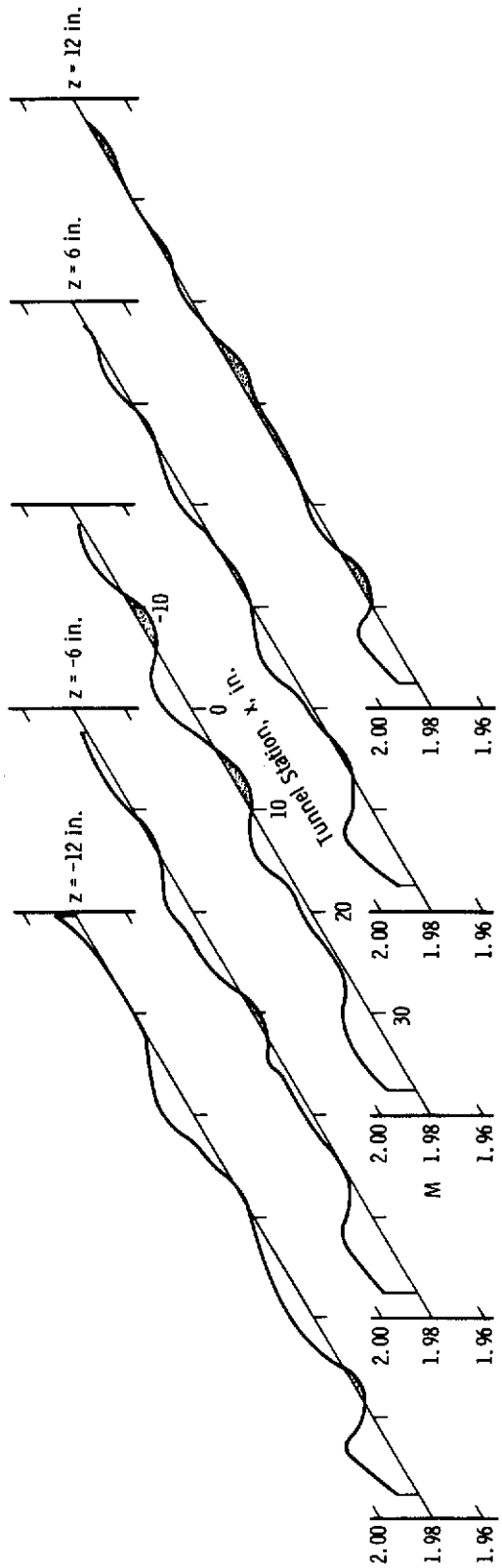

b. $M_c = 2$, $Re = 0.34 \times 10^6$

Fig. 8 Continued

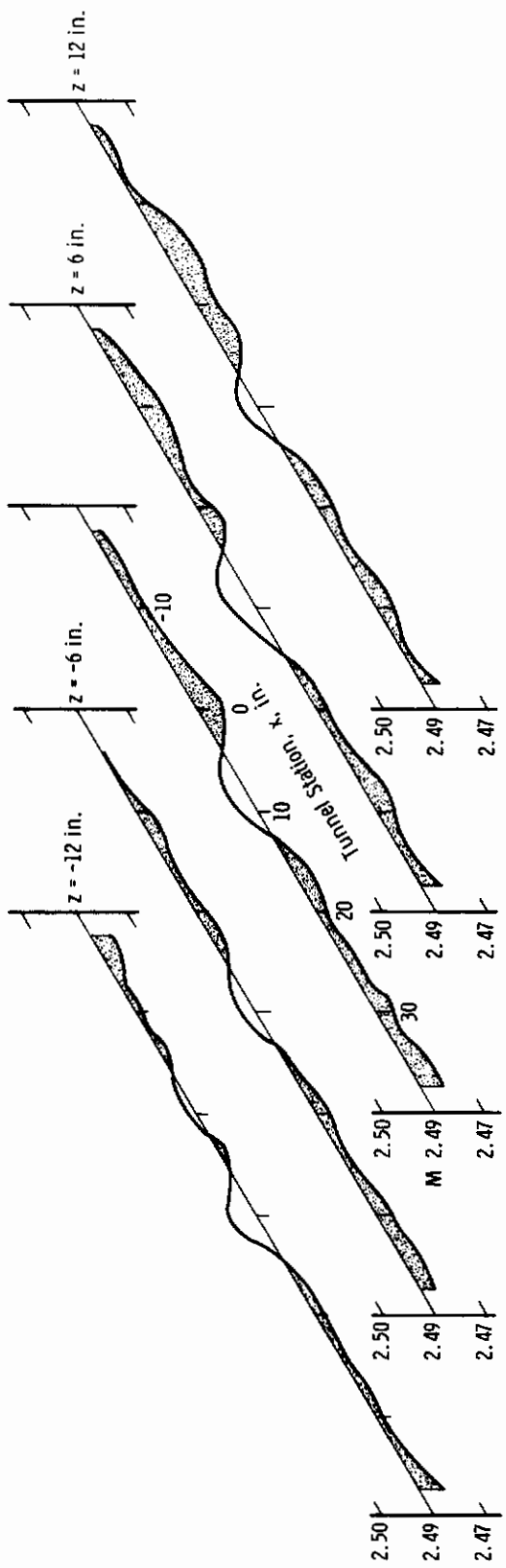

c. $M_c = 2.5$, $Re = 0.50 \times 10^6$

Fig. 8 Continued

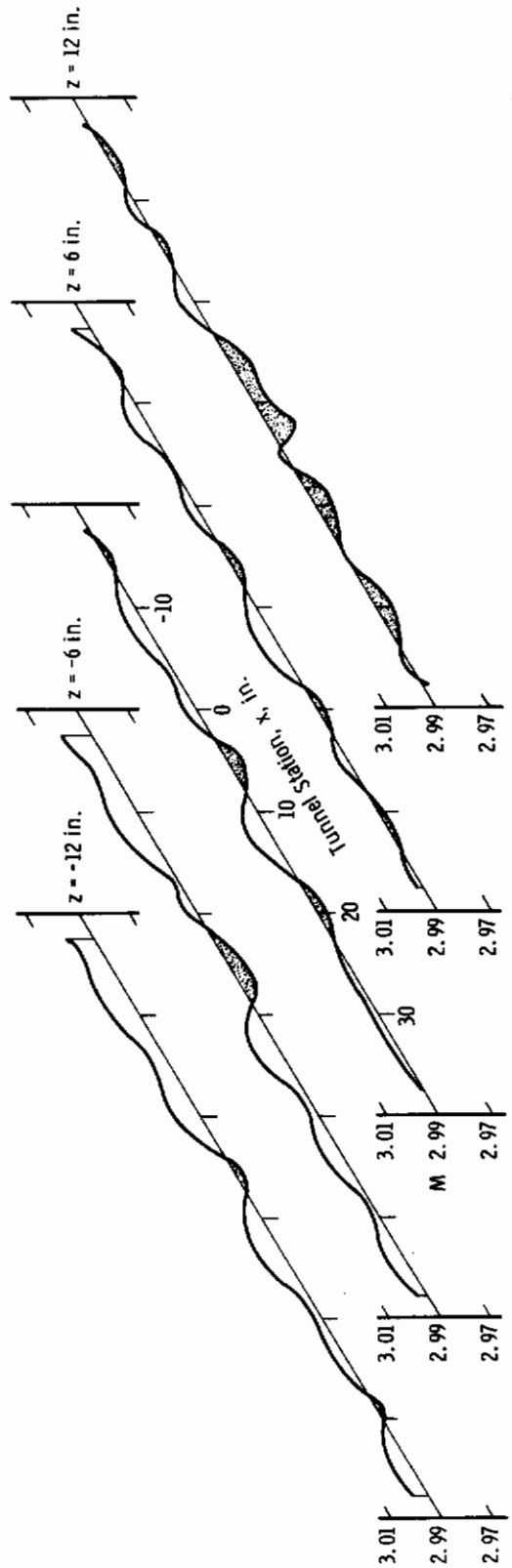

d. $M_c = 3$, $Re = 0.63 \times 10^6$

Fig. 8 Continued

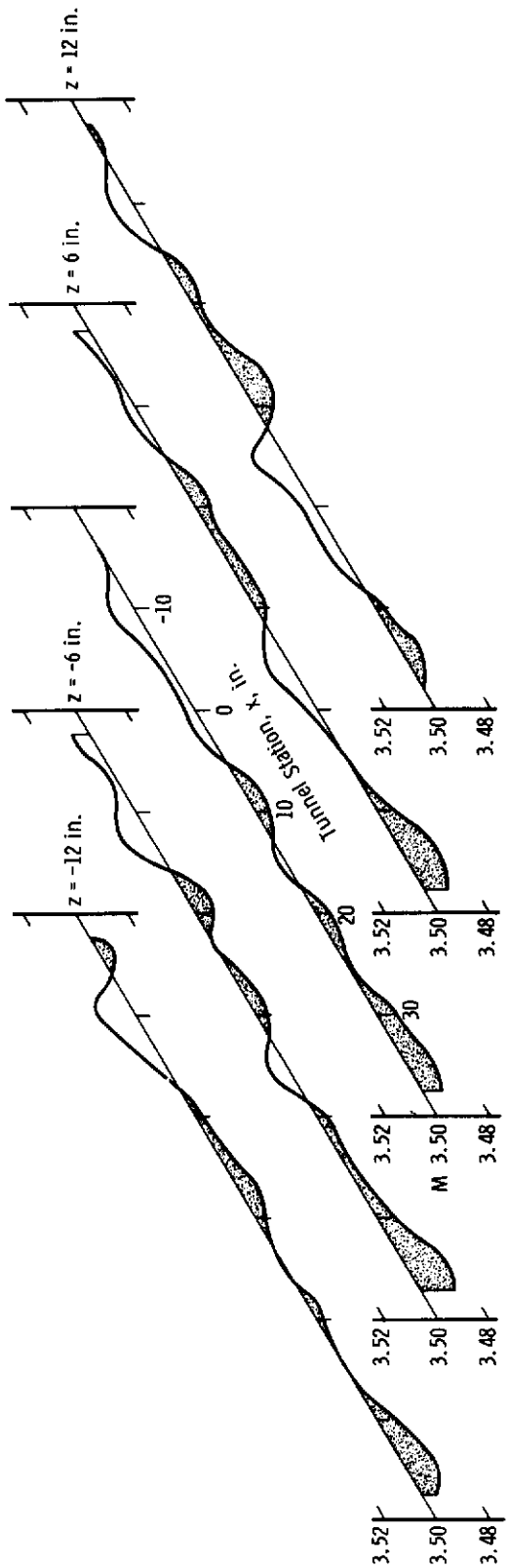

e. $M_c \approx 3.5$, $Re = 0.51 \times 10^6$

Fig. 8 Continued

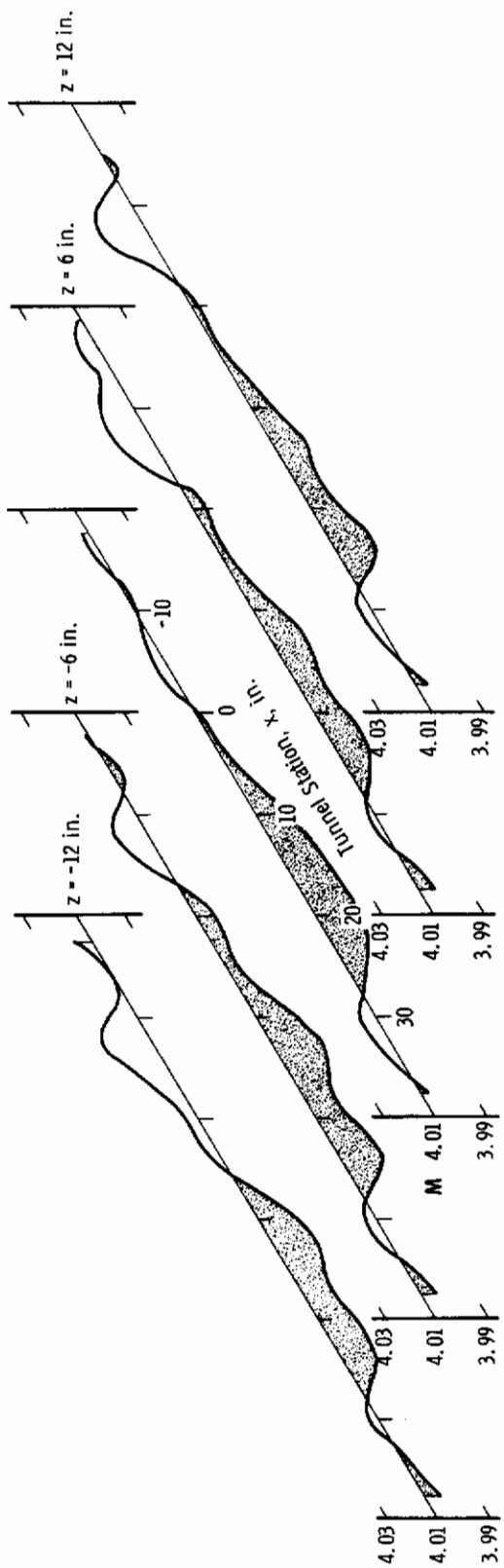

f. $M_c = 4$, $Re = 0.51 \times 10^6$

Fig. 8 Continued

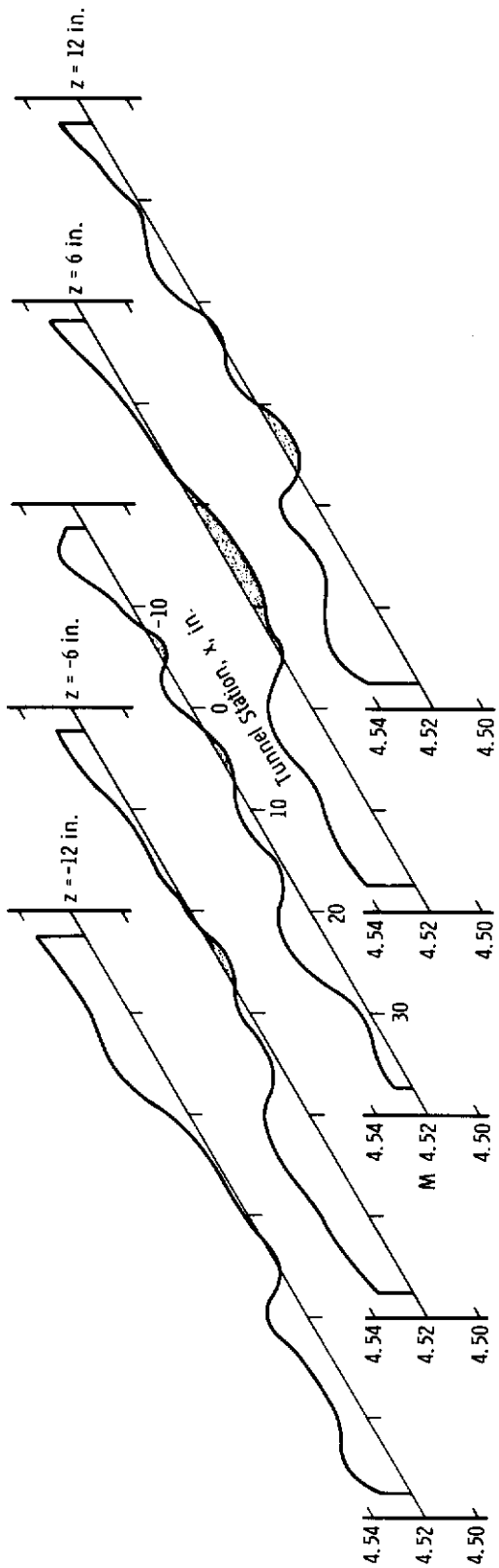

g. $M_c = 4.5$, $Re = 0.59 \times 10^6$

Fig. 8 Continued

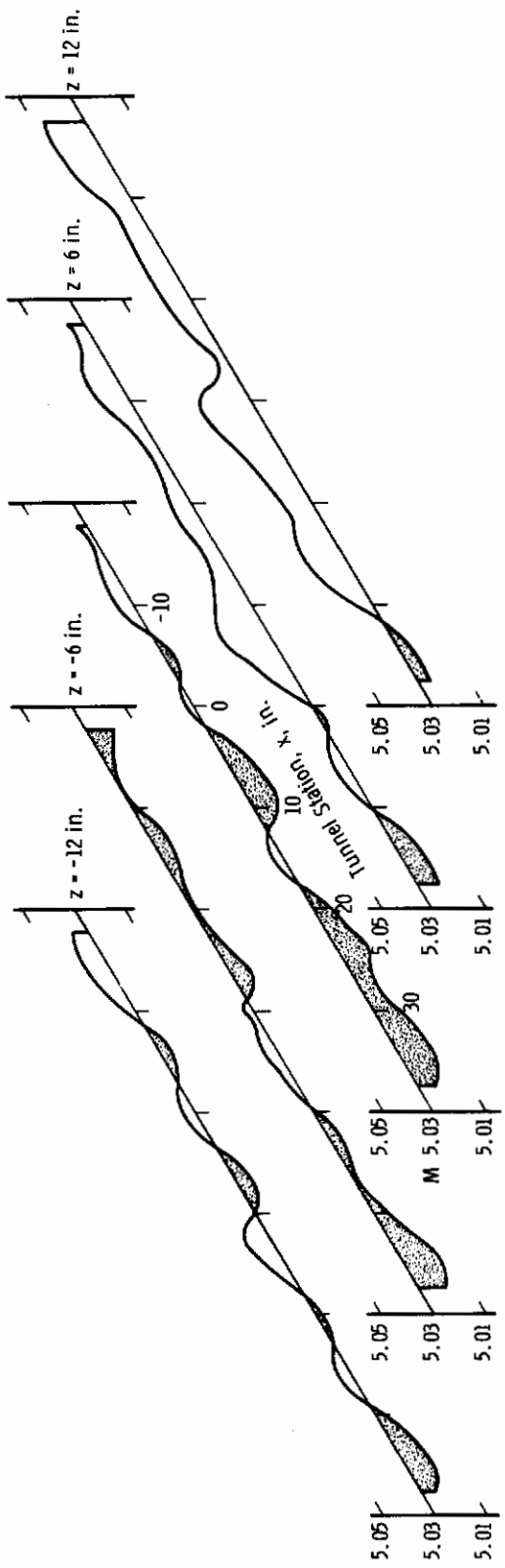

h. $M_c = 5$, $Re = 0.54 \times 10^6$

Fig. 8 Concluded

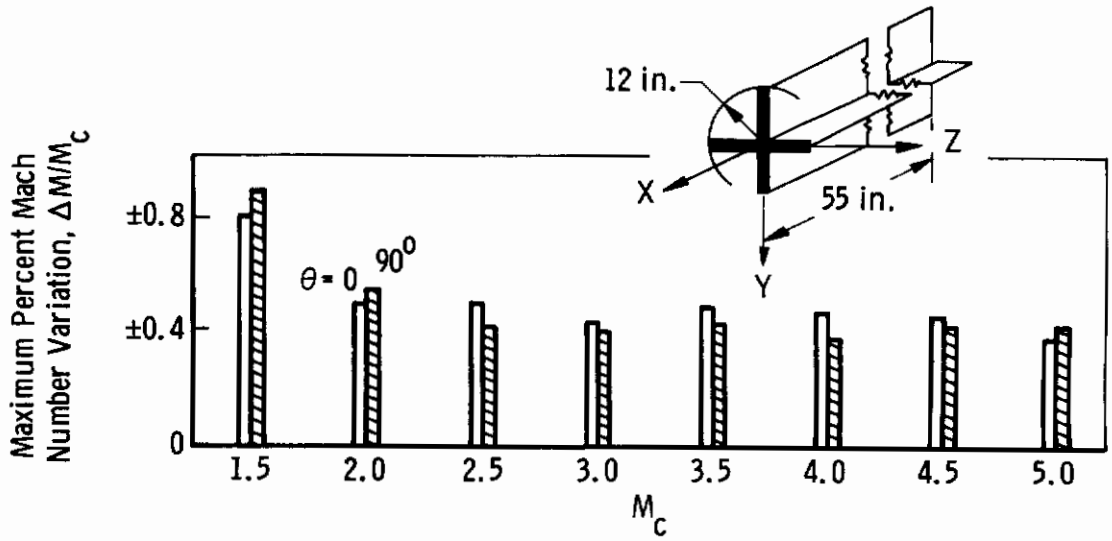

a. Mach Number Flow Nonuniformity within a Region of the Test Section

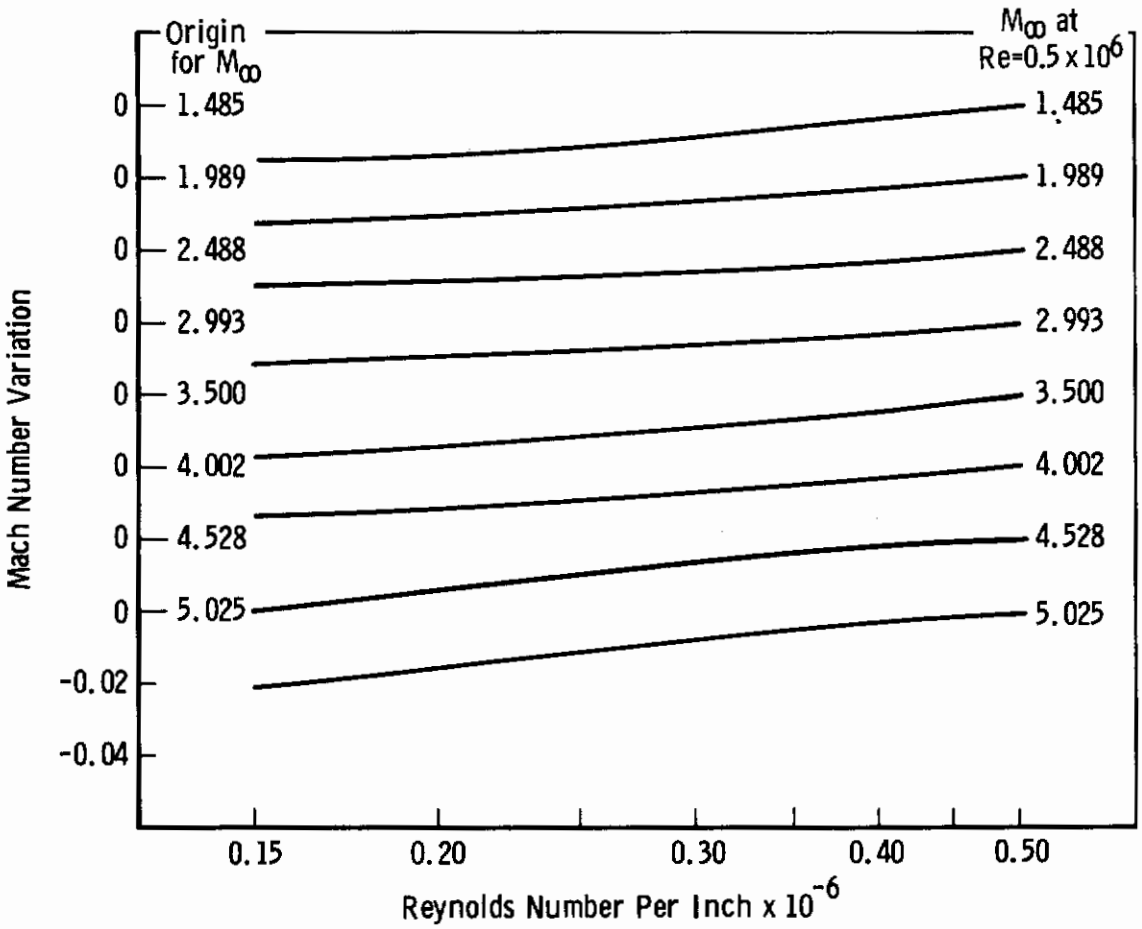

b. Variation of the Mean Centerline Mach Number with Reynolds Number

Fig. 9 Summary of Test-Section Mach Numbers from 1.5 to 5

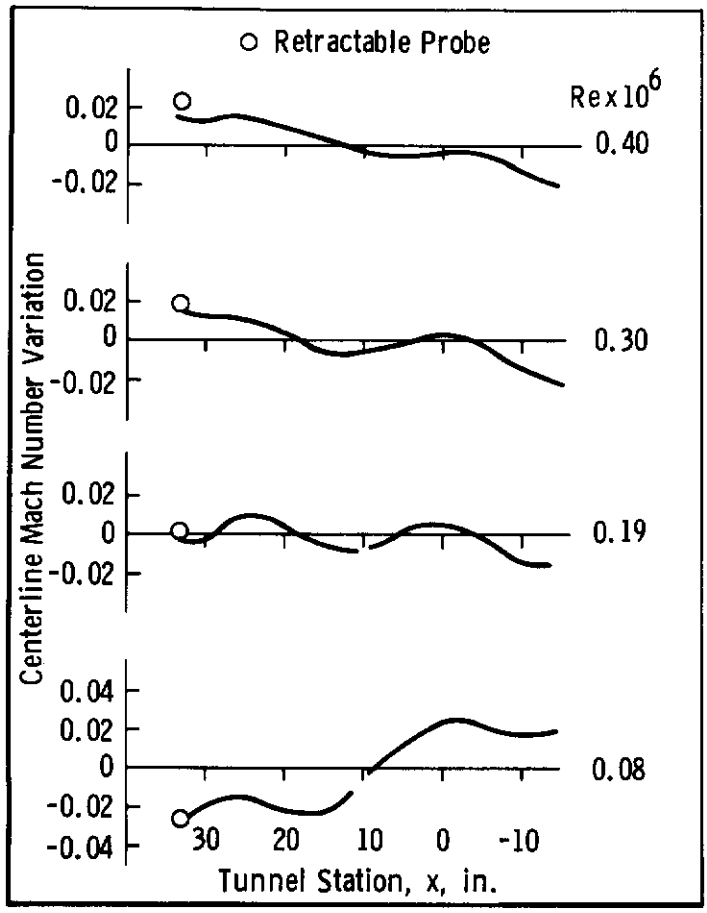

a. Centerline Mach Number Distribution about Mean Value at $M_c = 6$

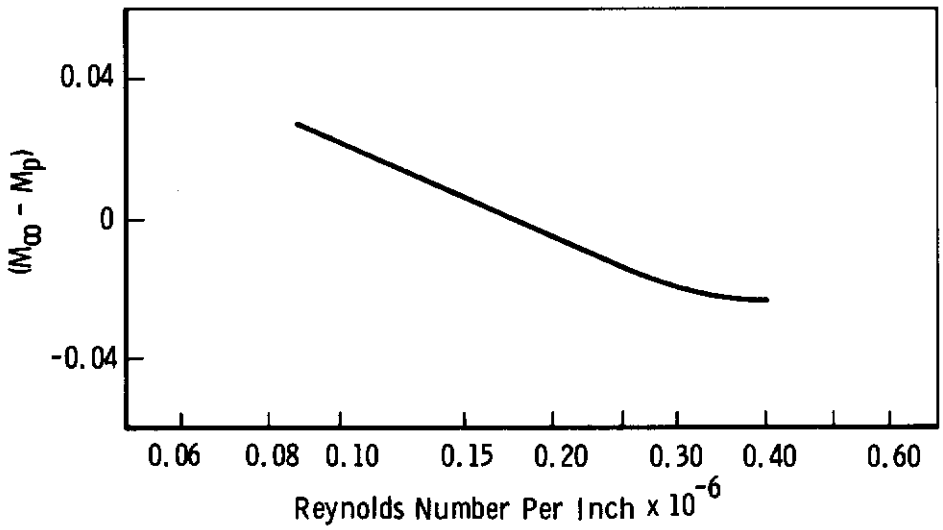

b. Variation of the Mach Number 6 Correlation Factor ($M_\infty - M_p$) with Reynolds Number

Fig. 10 Mach Number Characteristics at $M_c = 6$

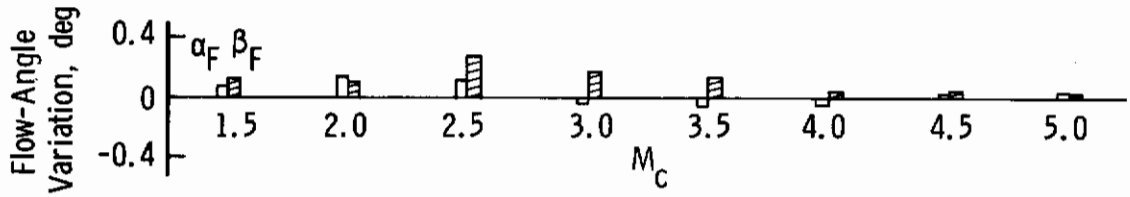

a. Mean Flow-Angle Variation along Tunnel Centerline

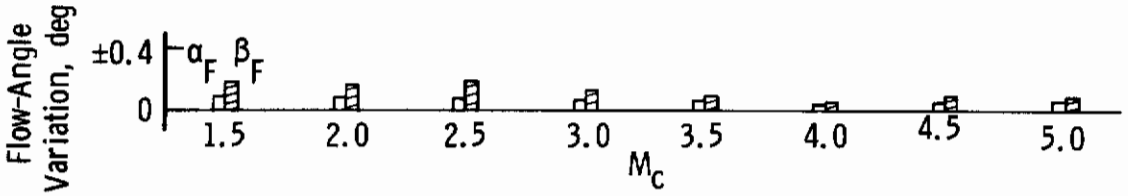

b. Maximum Flow-Angle Variation along Tunnel Centerline

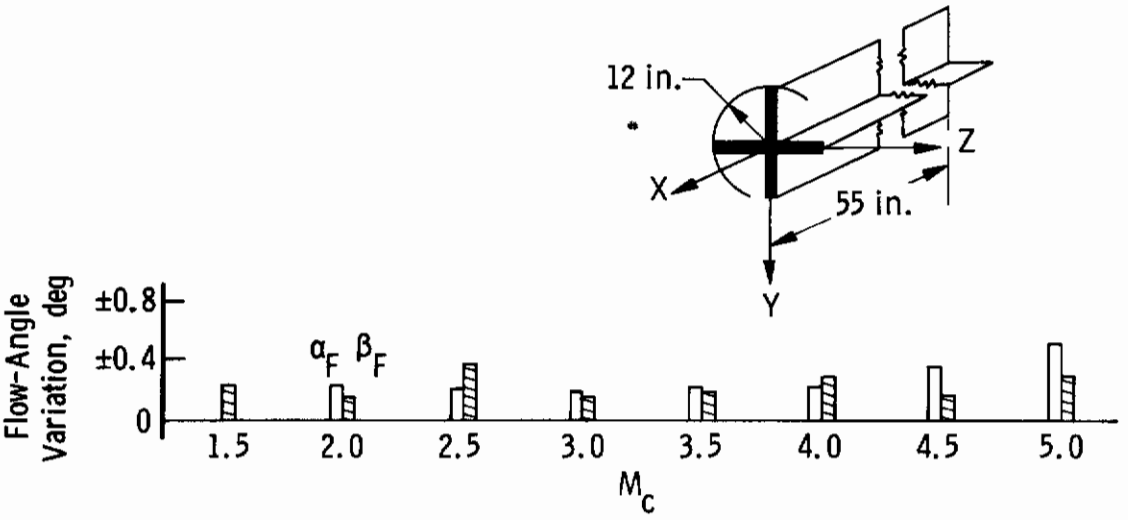

c. Maximum Flow-Angle Variation within a Region of the Test Section

Fig. 11 Summary of Test-Section Flow Angularity